Journal of
Applied Crystallography
ISSN 0021-8898

Received 6 July 2006
Accepted 18 August 2006

Enhancement of crystalline perfection by organic dopants in ZTS, ADP and KHP crystals as investigated by high-resolution XRD and SEM

G. Bhagavannarayana,[a]* S. Parthiban[b] and Subbiah Meenakshisundaram[b]

[a]Materials Characterization Division, National Physical Laboratory, New Delhi 110 012, India, and [b]Department of Chemistry, Annamalai University, Annamalai Nagar 608 002, India. Correspondence e-mail: bhagavan@mail.nplindia.ernet.in

To reveal the influence of complexing agents on crystalline perfection, tristhiourea zinc(II) sulfate (ZTS), ammonium dihydrogen phosphate (ADP) and potassium hydrogen phthalate (KHP) crystals grown by slow-evaporation solution growth technique using low concentrations (5×10^{-3} *M*) of dopants like ethylenediamminetetraacetic acid (EDTA) and 1,10-phenanthroline (phen) were characterized by high-resolution X-ray diffractometry (XRD) and scanning electron microscopy (SEM). High-resolution diffraction curves (DCs) recorded for ZTS and ADP crystals doped with EDTA show that the specimen contains an epilayer, as observed by the additional peak in the DC, whereas undoped specimens do not have such additional peaks. On etching the surface layer, the additional peak due to the epilayer disappears and a very sharp DC is obtained, with full width at half-maximum (FWHM) of less than 10 arcsec, as expected from the plane wave dynamical theory of X-ray diffraction for an ideally perfect crystal. SEM micrographs also confirm the existence of an epilayer in doped specimens. The ZTS specimen has a layer with a rough surface morphology, having randomly oriented needles, whereas the ADP specimen contains a layer with dendric structure. In contrast to ADP and ZTS crystals, the DC of phen-doped KHP shows no additional peak, but it is quite broad (FWHM = 28 arcsec) with a high value of integrated intensity, ρ (area under the DC). The broadness of the DC and the high value of ρ indicate the formation of a mosaic layer on the surface of the crystal. However, similar to ADP and ZTS, the DC recorded after etching the surface layer of the KHP specimen shows a very sharp peak with an FWHM of 8 arcsec. An SEM photograph of phen-doped KHP shows deep cracks on the surface, confirming the mosaicity. After removing the surface layer, the SEM pictures reveal a smooth surface. A similar trend is observed with other complexing agents, like oxalic acid, bipy and picolinic acid. However, only typical examples are described in the present article where the effects were observed prominently. The investigations on ZTS, ADP and KHP crystals, employing high-resolution XRD and SEM studies, revealed that some organic dopants added to the solution during the growth lead to the formation of a surface layer, due to complexation of these dopants with the trace metal ion impurities present in the solution, which prevents the entry of impurities, including the solvent, into the crystal, thereby assisting crystal growth with high crystalline perfection. The influence of organic dopants on the second harmonic generation efficiency is also investigated.

1. Introduction

In recent years, photonic devices have found increasing importance because of their unlimited information carrying, storage and processing capacity, cost effectiveness, *etc*. These devices require single crystals or fibres with nonlinear optical (NLO) properties (*e.g.* Huber, 1975). However, crystalline perfection plays an important role in device performance, which depends on the growth technique and conditions (Vijayan *et al*., 2006). Depending on the nature of the material, crystals can be grown conveniently only by certain methods. The slow-evaporation solution growth technique (SEST) is one of the well known, convenient, simple and cost-effective methods to grow many NLO crystals (Santhanaragavan &

Ramasamy, 2000). However, crystals grown by this technique are known to contain many impurities, including the solvent used in the method. Nevertheless, it is known that some complexing agents, when added to the solution, form complexes with impurities and enhance the metastable zone width and result in growth-promoting effects (Sangwal & Meilniczet-Brzoska, 2004; Meenakshisundaram *et al.*, 2006) when the complex absorption on the growing surface is not very stable. Chelating agents like ethylenediaminetetraacetic acid (EDTA), 1,10-phenanthroline (phen), oxalic acid, bipy, picolinic acid, *etc.*, are found to be good dopants in the rapid growth process due to their ability to complex with impurities, particularly the trace metal ions in the solution (Liu & Nancollas, 1973; Rajesh *et al.*, 2000; Kuboto, 2001; Pricilla Jeyakumari *et al.*, 2004; Li *et al.*, 2005; Anee *et al.*, 2005; Meenakshisundaram *et al.*, 2006). The resulting complex does not enter into the crystal, and also prevents the entry of impurities. However, no systematic studies had been carried out on the effect of such dopants on crystalline perfection. In the present study, using some chelating agents as dopants, the technologically important NLO crystals of tristhiourea zinc(II) sulfate (ZTS), ammonium dihydrogen phosphate (ADP) and potassium hydrogen phthalate (KHP), the structures of which were already known (Verma *et al.*, 2000; Veda & Sen, 1948; Okaya, 1965, respectively), were grown by the SEST method and the influence of the dopants on the crystalline perfection was investigated by employing nondestructive high-resolution X-ray diffractometry (XRD). Since the effect of chelating agents is prominent at the surface of the crystals, scanning electron microscopy (SEM) was used to assess the surface morphology. To reveal the influence of organic dopants on the second harmonic generation (SHG) conversion efficiency, which is one of the most important properties of NLO crystals, SHG measurements using an Nd:YAG laser source were also carried out.

2. Experimental details

2.1. Crystal growth

ZTS was synthesized (Arunmozhi *et al.*, 2004) by mixing zinc sulfate heptahydrate and thiourea in the stoichiometric ratio of 1:3. To avoid decomposition, low temperature (<346 K) was maintained during the preparation of the solution in deionized water. The product was purified by repeated recrystallization. For ADP and KHP, the commercially available raw materials were purified by repeated recrystallization. Crystals were grown by the SEST method. A very small quantity (5×10^{-3} *M*) of organic dopants was added to the aqueous solution. At these low concentrations of dopant, the growth-promoting effect is much greater than that observed in the absence of dopants or at their higher concentrations. Crystal growth experiments were carried out at 303 K in a constant-temperature bath under different acidic conditions at pH values in the range of 3.0 to 6.0. The pH variations were achieved using dilute sulfuric acid. The crystal growth rate and the quality of the crystals are much better when the solution is slightly acidic and the studies were mainly carried out at pH ~5.9. Under high acidity, the rate of crystal growth decreases considerably. At high concentration of the dopants, the adsorption film blocks the growth surface and inhibits the growth process as expected (Kuznetsov *et al.*, 1998). Solubility was analysed gravimetrically. The metastable zone width, which is a direct measure of the stability of the solution in its supersaturated region (Buckley, 1951), was measured by conventional polythermal method (Nyvlt *et al.*, 1970; Zaitseva *et al.*, 1995). The metastable zone width determined for doped material was found to be wider than that of pure material. In the presence of dopants, it was found that the secondary nucleation is also controlled to a considerable extent. With this method, good transparent crystals of ZTS, ADP and KHP with natural facets were grown. To understand the influence of dopants and to compare the crystalline perfection with undoped crystals, undoped crystals were grown under similar conditions.

2.2. High-resolution multicrystal X-ray diffractometry

To reveal the crystalline perfection of the grown crystals and to study the effect of chelating agents, a multicrystal X-ray diffractometer developed at NPL (Lal & Bhagavannarayana, 1989) was used to record high-resolution diffraction curves (DCs). In this system, a fine-focus (0.4 × 8 mm; 2 kW Mo) X-ray source energized by a well stabilized Philips X-ray generator (PW 1743) is employed. The well collimated and monochromated Mo $K\alpha_1$ beam obtained from the three monochromator Si crystals set in dispersive (+,−,−) configuration is used as the exploring X-ray beam. This arrangement improves the spectral purity ($\Delta\lambda/\lambda \ll 10^{-5}$) of the Mo $K\alpha_1$ beam. The divergence of the exploring beam in the horizontal plane (plane of diffraction) is estimated to be $\ll 3$ arcsec. The specimen crystal is aligned in the (+,−,−,+) configuration. Due to the dispersive configuration, though the lattice constant of the monochromator crystal(s) and the specimen are different, the unwanted dispersion broadening in the diffraction curve of the specimen crystal is insignificant. The specimen can be rotated about a vertical axis, which is perpendicular to the plane of diffraction, with minimum angular interval of 0.5 arcsec. The diffracted intensity is measured by using a scintillation counter.

2.3. Scanning electron microscopy

The surface morphology was observed using a LEO 440 scanning electron microscope in secondary electron imaging mode. SEM is an incredible tool for revealing the unseen world of micro space. It shows very detailed three-dimensional images at much higher magnification than is possible with an optical microscope. An electron gun (at the top) emits a beam of high-energy electrons. This beam travels downward through a series of magnetic lenses designed to focus the electrons to a very fine spot. As the electron beam hits each spot on the sample, secondary electrons are knocked loose from its surface. A detector counts these electrons and sends the

signals to an amplifier. The final image is built up from the number of electrons emitted from each spot on the sample.

2.4. Kurtz powder SHG measurements

The second harmonic generation test on the crystals was performed by the Kurtz powder SHG method (Kurtz & Perry, 1968). An Nd:YAG laser with modulated radiation of 1064 nm was used as the optical source and directed on the powdered sample through a filter. The grown crystals were ground to a uniform particle size of 125–150 μm and then packed in a microcapillary of uniform bore and exposed to laser radiation. The output from the sample was monochromated to collect the intensity of the 532 nm component and to eliminate the fundamental. Second harmonic radiation generated by the randomly oriented microcrystals was focused by a lens and detected by a photomultiplier tube. The doubling of frequency was confirmed by green radiation of 532 nm.

3. Results and discussion

3.1. High-resolution XRD and SEM studies

3.1.1. Undoped and EDTA-doped ZTS single crystals. To see the effect of dopants on the quality of ZTS single crystal, the DCs were recorded for undoped and doped crystals under the same conditions of X-ray power, beam height, *etc*. The curve (*a*) in Fig. 1 is the diffraction curve recorded for undoped ZTS single crystal for (001) diffracting planes. The curve contains a single peak with full width at half-maximum (FWHM) of 26 arcsec, which shows that the crystal does not contain any internal structural grain boundaries (Bhagavannarayana *et al.*, 2005) or an epitaxial layer (Bhagavannarayana & Halder, 2005), and the crystalline perfection is reasonably good. The curve (*b*) in Fig. 1 shows the DC for the EDTA-doped ZTS single crystal. As seen in the figure, the curve contains two peaks with an angular separation of 45 arcsec. The solid line is the convoluted curve of the two dotted curves, which is well fitted with the experimental points simulated by the Guassian curve fitting. To determine whether the additional peak is due to a low-angle structural grain boundary or some epilayer on the surface of the crystal, the surface of the specimen was lapped up to a few micrometres followed by chemical etching in a mixture of water and acetone in 1:2 ratio to remove the damaged surface resulting from the lapping.

The curve (*c*) in Fig. 1 shows the DC recorded after etching the same EDTA-doped specimen shown in Fig. 1(*b*). It is interesting to note that the satellite peak disappears after etching and the recorded diffraction curve is quite narrow with an FWHM of 6 arcsec, which is much less than that of undoped ZTS, *i.e.* 26 arcsec [curve (*a*)]. The FWHM value of 6 arcsec is very close to that expected from the plane wave theory of dynamical X-ray diffraction (Batterman & Cole, 1964). The single sharp diffraction curve with very low FWHM indicates that the crystalline perfection is extremely good. The specimen is a nearly perfect single crystal without having any internal structural grain boundaries and dislocations (or very low density of dislocations which could not be detected by high-resolution X-ray topography). Similar studies were carried out on benzene- and phen-doped ZTS crystals and the same trend was observed. These results indicate that complexation of trace metal ion impurities in the solution prevents the entry of impurities and thereby facilitates crystal growth with high crystalline perfection.

Fig. 2 shows the scanning electron micrographs recorded for the ZTS single-crystal specimens. The micrograph (*a*) depicts the surface features of the undoped specimen and shows a reasonably good uniform surface with some roughness, probably due to impurities. The picture (*b*) is of EDTA-doped ZTS crystal in its as-grown state. The micrograph suggests that

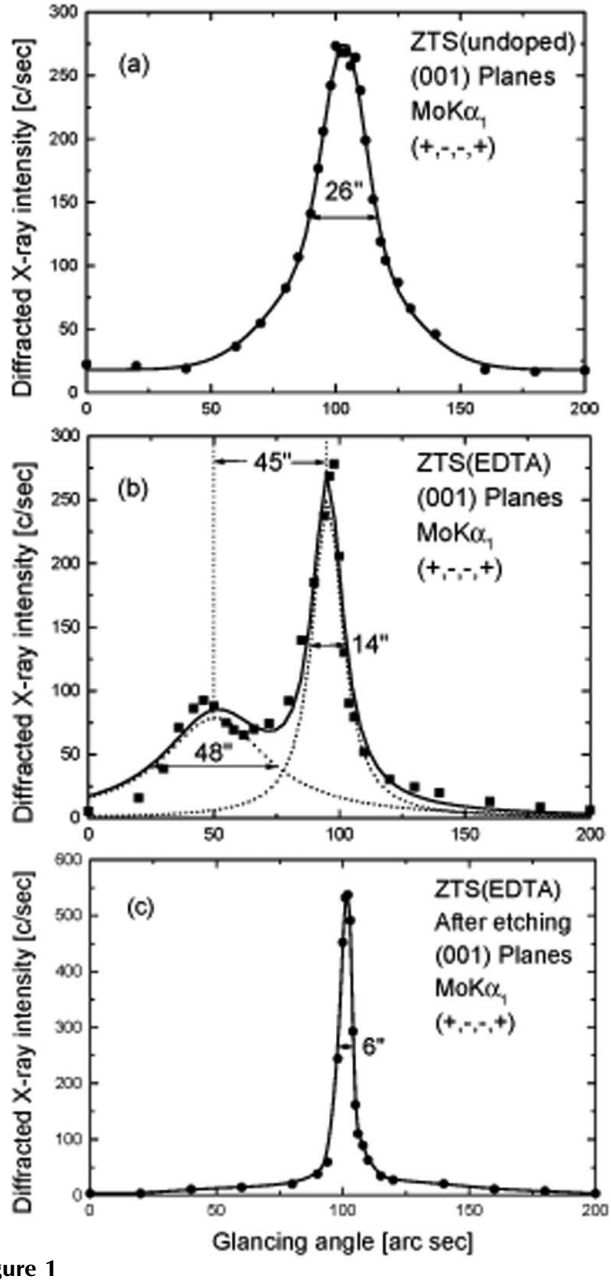

Figure 1
High-resolution X-ray diffraction curves recorded for ZTS single crystals: (*a*) undoped, (*b*) as-grown EDTA-doped and (*c*) after etching the surface layer of EDTA-doped specimens.

the specimen has a layer with a rough surface morphology having randomly oriented needles due to EDTA dopants. The micrograph (*c*) is of the same EDTA-doped specimen but after removing the surface layer by lapping followed by chemical etching. As seen in the picture, the surface is much smoother than that of (*b*). It is also smoother than that of micrograph (*a*), corresponding to the undoped specimen. These results confirm the formation of a surface layer where the impurities are absorbed, and are also in good agreement with the high-resolution XRD results.

To verify the effect of chelating agents on other crystals, ADP and KHP crystals were also grown and studied in the same manner as that of ZTS.

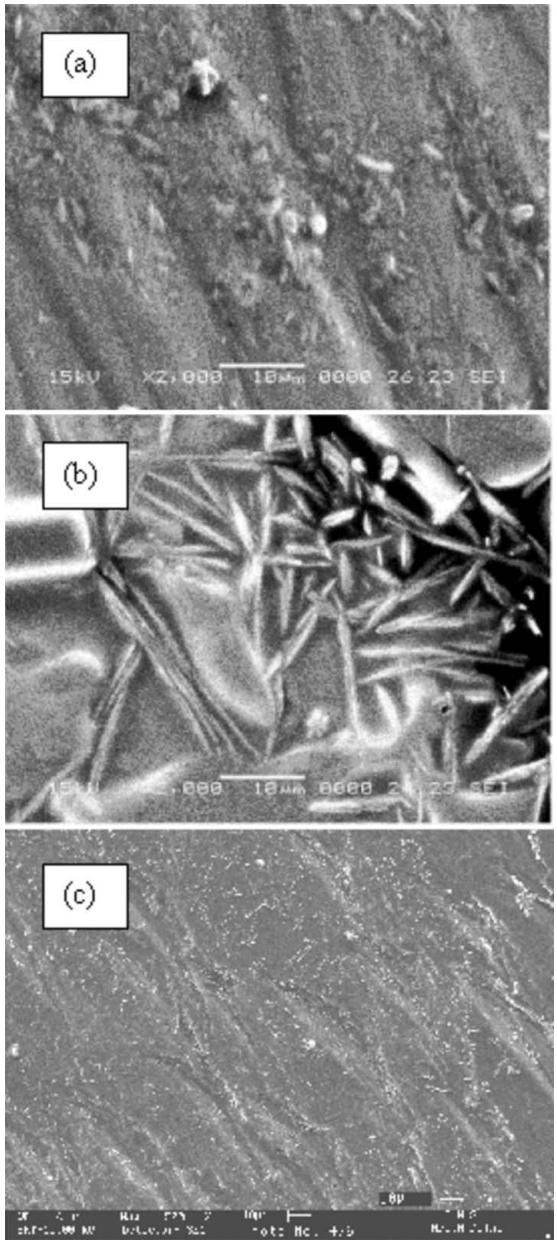

Figure 2
Scanning electron micrographs of ZTS single crystals: (*a*) undoped, (*b*) as-grown EDTA-doped and (*c*) after etching the surface layer of EDTA-doped specimens.

3.1.2. Undoped and EDTA-doped ADP single crystals. Fig. 3 shows the DCs recorded for undoped and doped crystals, in the same way as described for ZTS crystals, for (200) diffracting planes. Curve (*a*) shows the diffraction curve recorded for an as-grown ADP crystal without adding any chelating agent. As seen in the figure, the DC is quite sharp, having an FWHM of 11 arcsec, which indicates that the crystalline perfection is reasonably good. Curve (*b*) shows the DC recorded for an EDTA-doped ADP specimen. On the left-hand side of the curve, a shoulder can be observed which indicates that the specimen may contain an epitaxic layer. As in Fig. 1(*b*), the experimental DC was simulated with Guassian curve fitting. The solid line in the figure is the convolution of two peaks shown with dotted lines and is well fitted with the experimental points represented by the filled circles. This

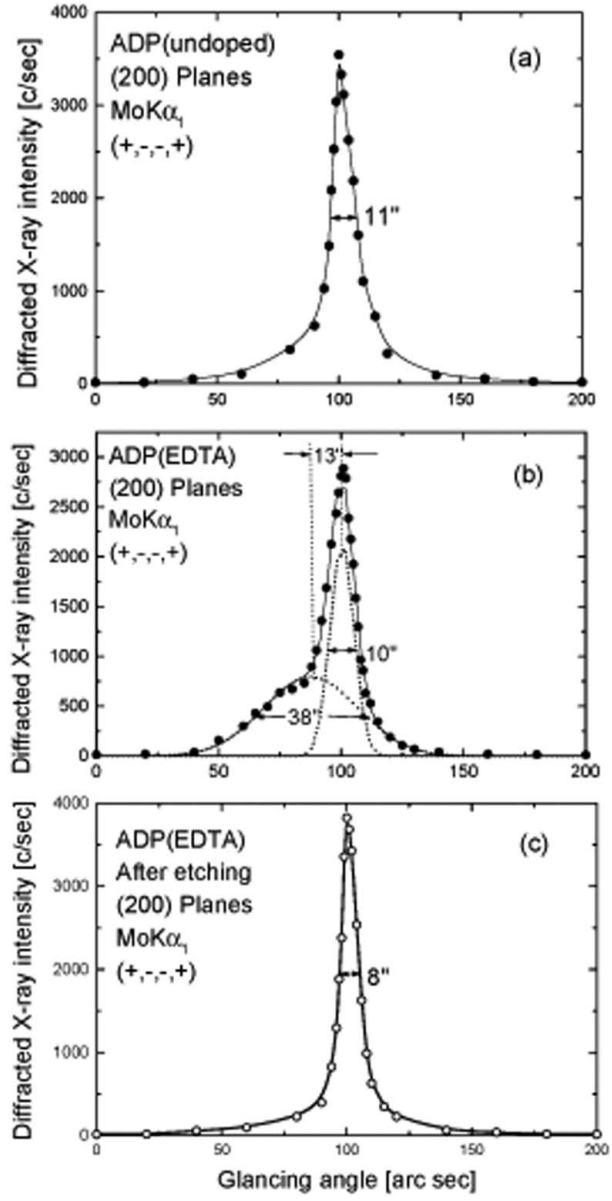

Figure 3
High-resolution X-ray diffraction curves recorded for ADP single crystals: (*a*) undoped, (*b*) as-grown EDTA-doped and (*c*) after etching the surface layer of EDTA-doped specimens.

indicates that the specimen contains an additional peak, which is 13 arcsec away form the main peak, having a broad half width of 38 arcsec. This additional peak could be either due to a film or due to a very-low-angle boundary. The surface of the same specimen crystal was chemically etched with a 1:2 ratio of water and acetone after lapping with fine alumina powder to remove a surface layer of a few micrometres thickness. Curve (*c*) shows the DC recorded after removing the surface layer. From the curve one can see that the shoulder has disappeared and the DC is very sharp, having a half width (FWHM) of 8 arcsec. Just as in the case of the EDTA-doped ZTS crystal, this observation clearly indicates that due to the chelating agent, a thin layer was formed on the surface of the crystal. The lower half width of curve (*c*) in comparison to that of curve (*a*) indicates that due to the presence of the chelating agent, the crystalline perfection has improved significantly. This example also indicates that complexation of trace metal ion impurities in the solution prevents the entry of impurities and thereby assists growth of the crystal with high crystalline perfection.

The SEM photographs for the ADP specimen crystals in their undoped, as-grown EDTA-doped and etched EDTA-doped (after removal of the surface layer) conditions are shown in Figs. 4(*a*), 4(*b*) and 4(*c*), respectively. The SEM picture of the as-grown EDTA-doped specimen shows dendric structure on the surface. After removing the surface layer, the SEM picture shows a relatively smoother surface of the crystal. Therefore, the SEM results are in good agreement with high-resolution XRD results, confirming the formation of a complexing surface layer by EDTA dopants with impurities.

3.1.3. Undoped and phen-doped KHP single crystals. Curve (*a*) in Fig. 5 is the diffraction curve recorded for an as-grown KHP crystal, without adding any chelating agent, for (010) diffracting planes. As seen in the figure, the DC is quite sharp, having an FWHM of 13 arcsec, which indicates that the crystalline perfection is reasonably good. Curve (*b*) shows the DC recorded using the phen agent with 5×10^{-3} *M* concentration. As seen in the figure, in contrast to ADP and ZTS crystals, the DC of phen-doped KHP shows no additional peak, but it is quite broader than curve (*a*), having an FWHM of 28 arcsec. The intensity along the wings of the curve on both sides of the diffraction peak position is also very high. One may notice that the intensity at angular distances of up to 100 arcsec with respect to the peak position does not decrease to zero, which is commonly expected for any reasonably good quality crystal even though its FWHM may be of the same order (*i.e.* around 28 arcsec). The integrated intensity, ρ, *i.e.* the area under the curve, is nearly 2.7 times that of the undoped specimen [curve (*a*)]. The broadness of the DC and the high value of ρ indicate that a mosaic layer on the surface of the crystal formed due to complexation of impurities in the solution with phen dopant. It may be mentioned here that ρ for ideally imperfect or mosaic crystals is proportional to the square of the structure factor (F_{hkl}^2), whereas for ideally perfect single crystals, it is proportional to the structure factor (F_{hkl}) and hence ρ is higher for imperfect crystals than for relatively perfect crystals (James, 1950). To confirm whether the mosaicity is limited to the surface, the surface has been lapped with fine alumina powder up to a few hundred micrometres, followed by chemical etching with a mixture of water and acetone in 1:2 ratio to remove the surface damage caused during lapping.

Curve (*c*) shows the DC recorded after removing the surface layer. From the curve, one can see that similar to curves (*c*) of Figs. 1 and 3 for the etched specimens of ZTS and ADP, respectively, the DC is very sharp, having an FWHM of

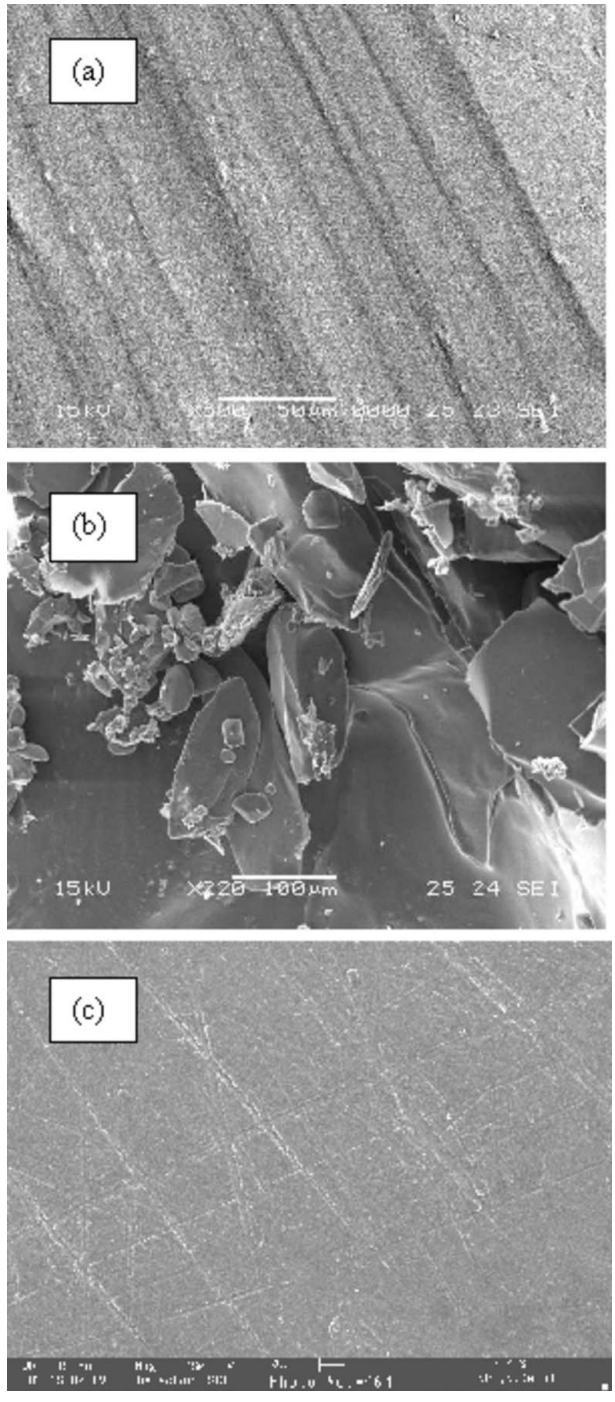

Figure 4
Scanning electron micrographs of ADP single crystals: (*a*) undoped, (*b*) as-grown EDTA-doped and (*c*) after etching the surface layer of EDTA-doped specimens.

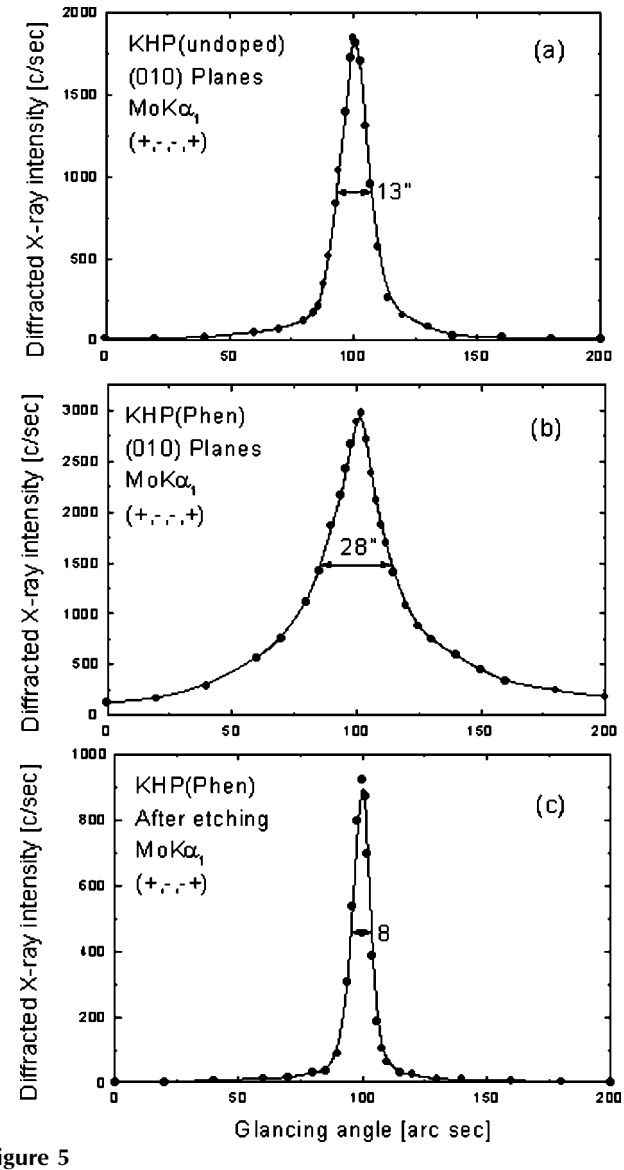

Figure 5
High-resolution X-ray diffraction curves recorded for KHP single crystals: (*a*) undoped, (*b*) as-grown phen-doped and (*c*) after etching the surface layer of phen-doped specimens.

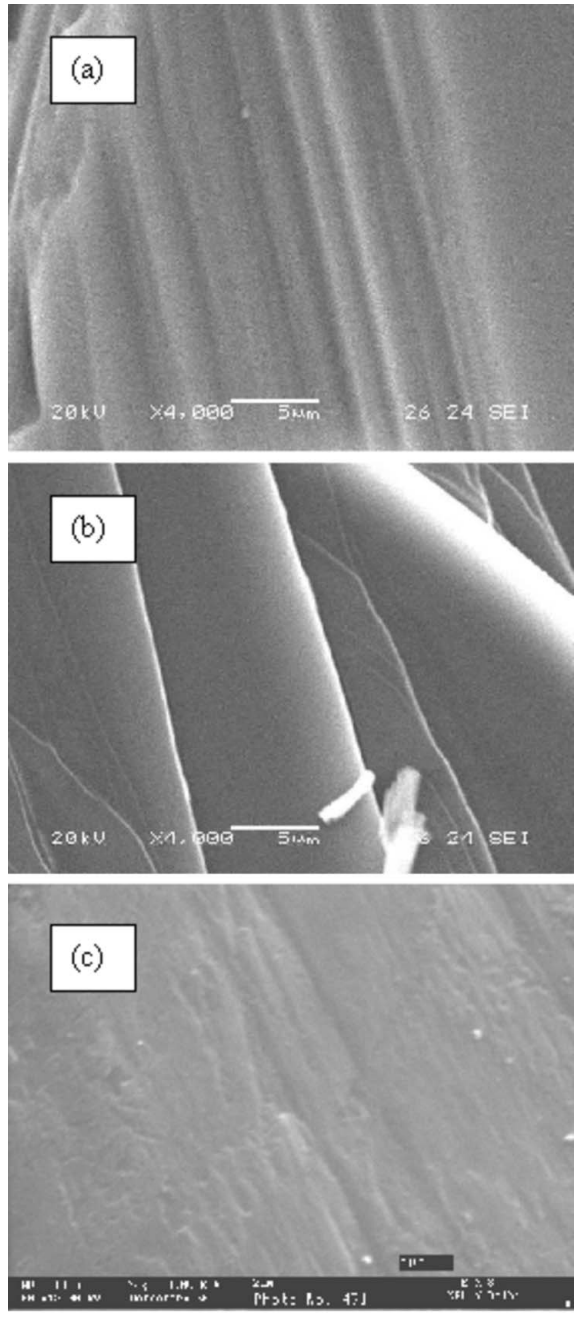

Figure 6
Scanning electron micrographs of KHP single crystals: (*a*) undoped, (*b*) as-grown EDTA-doped and (*c*) after etching the surface layer of EDTA-doped specimens.

8 arcsec. The single sharp DC with very low FWHM indicates that the crystalline perfection is much better than that of as-grown doped specimens. The integrated intensity of this curve is reduced up to one tenth with respect to that of curve (*b*) and around one third relative to that of curve (*a*) of Fig. 3. These features clearly indicate that, due to the chelating agent, a thin mosaic layer due to complexation of organic dopants with impurities was formed on the surface of the crystal. The low value of the FWHM and integrated intensity of curve (*c*) in comparison with curves (*a*) and (*b*) indicate that due to the presence of the chelating agent, the crystalline perfection is improved significantly.

The SEM photographs for undoped KHP, as-grown phen-doped KHP and phen-doped KHP after removal of the surface layer are shown in Figs. 6(*a*), 6(*b*) and 6(*c*), respectively. SEM picture (*b*) of the as-grown phen-doped KHP specimen shows deep crack development on the surface, confirming the mosaicity as observed by high-resolution XRD. After removing the surface layer, the SEM picture (*c*) shows a very smooth surface of the crystal without any mosaicity. Therefore, the SEM results indicate that the mosaicity is limited to the surface. Therefore, for this specimen also, the high-resolution XRD results along with the SEM micrographs confirm that the complexation of impurities with the dopants restricts the entry of impurities inside the crystal during crystal growth.

Table 1
SHG output for undoped and doped ZTS, ADP and KHP crystals.

System	$I_{2\omega}$ (mV)
ZTS	48–49
ZTS/EDTA	89–91
ADP	500–600
ADP/EDTA	600–700
KHP	163–165
KHP/phen	136–138

From the above three typical illustrative examples, and also from similar observations with other additives, like oxalic acid, bipy and picolinic acid, one can conclude that the presence of some suitable complexing agent improves the crystalline perfection to a great extent, as indicated by the reduction of FWHM and integrated intensity values. At the same time, these agents promote the growth process, leading to rapid growth with high crystalline quality.

3.2. SHG efficiency

As described in §2.4, an SHG test on the powder samples was performed by the Kurtz powder SHG method. The input radiation was 5 millipoize pulse^{-1}. The output SHG intensities for pure and doped specimens give relative NLO efficiencies of the measured specimens. These values are given in Table 1. EDTA as dopant enhances the NLO efficiency of ZTS and ADP; this is in tune with the relatively high magnitude of crystalline perfection observed, as indicated by single and sharp diffraction curves for the bulk crystals after removing the surface layer. Depressed SHG output in the case of phen dopant is quite likely due to the disturbance of charge transfer (Meenakshisundaram *et al.*, 2006). It appears that because of the orientational cancellation, the second-order susceptibility for SHG vanishes.

Although many materials have been identified that have higher molecular nonlinearities, the attainment of second-order effects requires favourable alignment of the molecule within the crystal structure (Hall *et al.*, 1986). To elaborate, efficient SHG demands specific molecular alignment of the crystal to be achieved, facilitating nonlinearity, in the presence of a dopant. It has been reported that the SHG can be greatly enhanced by altering the molecular alignment through inclusion complexation (Ying & Eaton, 1985).

4. Conclusions

Enhancement of crystalline perfection due to suitable organic dopants in different NLO crystals has been clearly demonstrated by employing high-resolution XRD. These studies also reveal that a less adsorbent surface layer forms through the complexation of impurities with dopants and thereby prevents the entry of impurities into the bulk crystal lattice. SEM studies confirm the formation of a complexing surface layer. Improvement in the crystalline perfection due to reduction of impurities leads to improvement in SHG efficiency in ZTS and ADP crystals. However, the dopant phen in the case of KHP depresses the SHG efficiency, which may be rationalized by envisaging an unfavourable molecular alignment affecting the nonlinearity.

One of the authors (GB) is grateful to Dr Vikram Kumar, Director, NPL, and Dr S. K. Gupta, Head, Materials Characterization Division, for their kind support and encouragement in carrying out the present studies. The authors are thankful to Shri K. N. Sood for recording the scanning electron micrographs.

References

Anee, T. K., Meenakshisundaram, N., Arivuoli, D., Ramasamy, P. & Narayana Kalkura, S. (2005). *J. Cryst. Growth.* **285**, 380–387.
Arunmozhi, G., Gomes, E. dem & Ganesamoorthi, S. (2004). *Cryst. Res. Technol.* **39**, 408–413.
Batterman, B. W. & Cole, H. (1964). *Rev. Mod. Phys.* **36**, 681–717.
Bhagavannarayana, G., Ananthamurthy, R. V., Budakoti, G. C., Kumar, B. & Bartwal, K. S. (2005). *J. Appl. Cryst.* **38**, 768–771.
Bhagavannarayana, G. & Halder, S. K. (2005). *J. Appl. Phys.* **97**, 024509(1–6).
Buckley, H. E. (1951). Editor. *Crystal Growth*. New York: Wiley.
Hall, S. R., Kolinsky, P. V., Jones, R., Allen, S., Gordon, P., Bothwell, B., Bloor, D., Norman, P. A., Hursthouse, M., Karaulor, A. & Baldwin, J. (1986). *J. Cryst. Growth*, **79**, 745–751.
Huber, P. (1975). *Optics Commun.* **15**, 196–200.
James, R. W. (1950). *The Optical Principles of the Diffraction of X-rays*, p. 271. London: G. Bell.
Kuboto, N. (2001). *Cryst. Res. Technol.* **36**, 749–769.
Kurtz, S. K. & Perry, J. J. (1968). *J. Appl. Phys.* **39**, 3798–3813.
Kuznetsov, V. A., Okhrimenko, J. M. & Rak, M. (1998). *J. Cryst. Growth.* **193**, 164–173.
Lal, K. & Bhagavannarayana, G. (1989). *J. Appl. Cryst.* **22**, 209–215.
Li, G., Xue, L., Su, G., Li, Z., Zhuang, X. & He, Y. (2005). *Cryst. Res. Technol.* **40**, 867–870.
Liu, S.-T. & Nancollas, G. H. (1973). *J. Colloid Interface Sci.* **44**, 422–429.
Meenakshisundaram, S., Parthiban, S., Sarathi, N., Kalavathy, R. & Bhagavnnarayana, G. (2006). *J. Cryst. Growth.* **293**, 376–381.
Nyvlt, J., Rychly, R., Gottfried, J. & Wurzelova, J. (1970). *J. Cryst. Growth.* **6**, 151–162.
Okaya, Y. (1965). *Acta Cryst.* **19**, 879–882.
Pricilla Jeyakumari, A., Ramajothi, J. & Dhanuskodi, S. (2004). *J. Cryst. Growth.* **269**, 558–564.
Rajesh, N. P., Meera, K., Srinivasan, K., Santhana Raghavan, P. & Ramasamy, P. (2000). *J. Cryst. Growth*, **213**, 389–394.
Sangwal, K. & Meilniczet-Brzoska, E. (2004). *J. Cryst. Growth*, **267**, 662–675.
Santhanaragavan, P. & Ramasamy, P. (2000). *Crystal Growth Methods and Process*. Kumbakonam, India: Kuru Publications.
Veda, R. & Sen, X. (1948). *X-rays*, **5**, 21.
Verma, S., Singh, M. K., Wadhawan, V. K. & Suresh, C. H. (2000). *J. Phys.* **54**, 879–888.
Vijayan, N., Bhagavannarayana, G., Ramesh Babu, G., Gopalakrishnan, R., Maurya, K. K. & Ramasamy, P. (2006). *Cryst. Growth Des.* **41**, 784–789.
Ying, W. & Eaton, D. F. (1985). *Chem. Phys. Lett.* **120**, 441–444.
Zaitseva, N. P., Rashkovich, L. N. & Bogatyreva, S. V. (1995). *J. Cryst. Growth*, **148**, 276–282.